A Complex System Model of Glucose Regulatory Metabolism

Perambur S. Neelakanta*
Meta Leesirikul
Zvi Roth
Salvatore Morgera
Department of Electrical Engineering,
Florida Atlantic University,
Boca Raton, Florida 33431

Consistent with inherent characteristics of a complex system made of a large number of interacting units having deterministic as well as spatiotemporal attributes, a model is developed to represent the human glucose regulatory metabolism within a complex system framework. Essentially, the mass-flow relations pertinent to sugar transport (in the form of glucose), and sugar regulatory hormones (namely, insulin and glucagon) across various participant parts of the body are depicted as nonlinear (logistic) functions; and hence, the temporal growth of blood plasma glucose concentration as well as the rate of change of such concentration levels are derived and expressed in terms of a Bernoulli–Langevin expression, (which functionally depicts the associated nonlinearity whose spatial order is implicitly dictated by the underlying complexity of the processes involved). Simulated results based on theoretical formulations derived are validated with respect to available clinical data due to Cobelli and Mari [1, 2], whose deterministic model of mass-balance relation pertinent to glucose regulatory metabolism is modified and adapted into complex system considerations. The results illustrate the statistical spread with upper and lower bounds associated with the temporal excursions of glucose concentration and its rate of appearance in blood plasma. The outcome of this study, for example, can find applications in refining predictive control algorithms adopted in closed-loop glucose control regimens (*via* insulin infusion pumping) prescribed to maintain normoglycemia in Type I diabetic patients.

1. Introduction

This paper proposes a strategy towards modeling human glucose regulatory metabolism *in vivo* [2, 3] in terms of system complexity, which is subjected for validation using observed data [1, 2]. The motivation for such a model is the need to elucidate realistic statistical bounds within

*Electronic mail address: neelakan@fau.edu.

Complex Systems, **16** (2006) 343–367; © 2006 Complex Systems Publications, Inc.

https://doi.org/10.25088/ComplexSystems.16.4.343

which such a regulatory process can be traced along the time scale. An example use of these bounds is to design external methods of infusing insulin in diabetic patients [4–6] and monitoring the associated regulation within (tolerable) upper and lower bounds.

In this paper the metabolic system and associated activities are regarded as subset entities of a complex spatiotemporal system, which from an observer's standpoint consists of a statistically large number of interacting units whose functions are directed towards a global objective [7, 8]. The set of such units in general, refers to different compositions (mixes) of structural (spatial) entities having a functional behavior that varies within the associated dynamics. Further, the system depicts a large stochastical domain (in space and time) with random attributes; hence, the constituent units can be characterized largely in terms of spatiotemporal statistical norms pertinent to interaction mechanics in the universe of a complex system domain.

In short, this paper is intended to formulate a complex system model of metabolic activity of physiological interest. For analysis purposes we specifically consider an example system that depicts the glucose regulatory process, which is assumed to have deterministic and/or stochastical attributes. The proposed model aims to predict and infer temporal excursions of the variables of interest (in terms of mostly dormant subsets of related variables in the physio-anatomical system). The outcome of this study is projected to indicate the statistical (upper and lower) bounds on temporal excursions of blood-glucose concentration and the rate of appearance of glucose in blood plasma as regulated by the hormonal participants insulin and glucagon. The simulated results in this study are validated and compared against available clinical data [1, 2].

The approach pursued can lead to modifying/tuning model components within the statistical bounds established. Such modifications are useful, for example, to refine predictive control algorithms adopted in closed-loop glucose control regimens (administered *via* insulin infusion pumping) for maintaining normoglycemia in Type I diabetic patients [4–6].

2. Complex system considerations

Regulatory mechanisms in biological systems such as glucose regulation can be assumed as embodiments of a complex system made of heterogeneous constituents with statistical functional attributes, which are mostly intertwined.

In general, such a complex system can be specified by a metric, which represents a generalized estimate of complexity *vis-à-vis* the constituent entities, their stochastical attributes, their functions, and their temporal dynamics. Therefore, in a spatiotemporal domain, this *metric of*

complexity (C) can be defined as follows [7, 8]:

$$C(t) = \varphi\{n(t), N(t)\} \tag{1}$$

where n is the countable number of (large) constituent elements, N is their variety, and t denotes the time. Further, ϕ is a function that has to be modeled so that $C(t)$ denotes the extent (measure) of complexity involved consistent with the details of a good fit on experimental observations. In general, n and N, as well as their dynamics (with respect to time) can be deterministic and/or stochastical.

In a biological regulatory process, the complexity (C or ϕ) may depict a disorderly state at some reference time, say $t = 0$. The regulatory process strives *via* feedback to achieve a desired regulation. That is, the associated cybernetics seeks the objective function (specifying the goal) towards realizing an orderliness at a later instant of time [7, 8] reducing thereby the entropy of the system.

3. Glucose regulation model

Metabolism signifies any reaction that takes place within the living system. Such reactions normally involve both energy-releasing and energy-consuming processes [9]. *Glucose metabolism* specifically refers to the metabolic reaction of glucose, that is, the way it is metabolized, stored, and used by various parts of the body.

There are four main sinks for glucose in the bloodstream as destination sites [4] where either the glucose is metabolized/stored or excreted. These locations are as follows.

- Insulin-sensitive cells (ISCs) where glucose is metabolized.
- Noninsulin-sensitive cells (NISCs) are other sites where glucose is metabolized.
- The kidneys are where glucose is lost due to excretion *via* urine.
- Liver or muscle cells are where glucose is stored.

We now summarize some explanatory notes on these glucose sinks.

Muscle cells are ISCs where the rate of glucose diffusion depends on the level of muscular activity, for example, more glucose is metabolized in these cells when exercising. This metabolism leads to a decrease in the level of glucose in intracellular fluid causing an increase in the concentration gradient of glucose across the membrane separating intra- and extracellular domains. Glucose diffusion into the cells is promoted by insulin, which facilitates the entrance of glucose crossing the cell membrane into the cell interior (where the glucose is metabolized).

In other cells such as nerve tissues, the rate of glucose diffusion into the cell would occur even in the absence of insulin and the diffusion rate is proportional only to the glucose concentration gradient.

https://doi.org/10.25088/ComplexSystems.16.4.343

Glucose will be excreted *via* urine through the kidneys when the level of glucose in blood plasma rises above a threshold value ($\approx$1.76 mg/ml). The relevant mechanism is controlled by renal filtration caused by the blood pressure in a tuft of capillaries in the kidney (known as the *glomerulus*) forcing plasma to exert the filtration of dissolved materials and small proteins. When the filtration rate exceeds the rate of glucose absorption into the plasma stream, then the excess glucose becomes unusable and is excreted *via* urine.

With reference to the given details on glucose, the main sources of glucose in dictating the associated regulation metabolism are:

- dietary intake
- stored fat and protein
- glycogen.

The salient features of these sources of glucose are outlined below.

Under normal health conditions, prior to dietary-intake (or during starvation), the glucose level may go down as a result of reduced availability of ingested glucose. This condition is known as *hypoglycemia*. Also, due to physical exercise/stress, the glucose level may fall as a result of utilizing the available glucose. Likewise, the glucose level may rise after food intake, a condition known as *hyperglycemia*. (The level of glucose in the bloodstream at a required base level has to be kept up so as to serve as fuel for the cells [known as maintaining "cell respiration"].)

The hypo- or hyperglycemic states are mediated mainly by the pancreas and liver. The pancreas is the site of what are known as pancreatic islets (*islets of Langerhans*), where two types of cells called *alpha-* and *beta-cells* exist. These cells secrete two vital hormones needed for glucose regulation. The alpha-cells secrete the so-called *glucagon* hormone and the beta-cells are responsible for secreting the well-known *insulin* hormone.

The roles played by glucagon and insulin in the regulatory metabolism in question now follows. As mentioned earlier, insulin mediates the transport of glucose from the bloodstream into the cell bodies (except in NISCs) by increasing the permeability of cell membranes to glucose.

Absorption of carbohydrates in the intestinal tract (e.g., after eating a high carbohydrate meal) and the resulting gush of glucose would cause blood-glucose concentration to rise above its normal level of 80 to 90 mg/100ml. Under such hyperglycemic conditions, the beta-cells become active and make insulin to circulate so that insulin-dependent cells use up the glucose entering them as fuel. This process continues until the blood sugar level returns to a normal baseline from the high hyperglycemic level. (Apart from its glucose controlling function, insulin also plays the role of using certain fatty and amino acids to synthesize lipids and proteins.)

Some glucose available from food intake, and subsequently present in the bloodstream, is also converted into *glycogen* (an extensively branched glucose polysaccharide depicting an animal equivalent of starch) compatible for storage and later usage. This glycogen production (or *glycogenesis*) occurs in the liver and in skeletal muscles. This muscle glycogen then breaks down to glucose phosphate and then into two molecules of pyruvic acid eventually releasing energy, which gets stored as high-energy ATP molecules. Another version of glycogen production also exists. This glycogenesis process occurs in the liver; and, the hormone glucagon (secreted by the alpha-cells of the pancreas) stimulates the liver to convert this glycogen back to glucose, which is then placed in the bloodstream. This process of breaking down glycogen back into glucose is called *glycogenolysis*. Glucagon also promotes the use of fats and excess amino acids (noncarbohydrate entities) for conversion into simple carbohydrates that would, in turn lead to new glucose production (known as *gluconeogenesis*). In the end, the glucose produced by different activities will enter, as needed, into relevant reactions of cell respiration towards energy production.

Thus, the overall function of glucagon is to raise the blood-glucose level and make all types of food available for energy production. That is, glucagon is secreted whenever hypoglycemic conditions occur (in contrast to insulin secretion, which happens under hyperglycemic situations). Thus, insulin and glycogen portray antagonistic functions in glucose regulatory metabolism as summarized in Figure 1.

In summary, control of glucose is crucial in maintaining sugar balance among the body parts. It implies proper carbohydrate, fat, and protein-based energy processes in the cells mediated by the glucose metabolism. In the event of abnormal glucose regulation, the pathological state of *diabetes mellitus* will occur. It is a syndrome of impaired carbohydrate, fat, and protein metabolism. That is, in a diabetic person, glucose uptake and utilization are not efficient. Since glucose largely circulates around in the plasma stream and a very small amount diffuses into intracellular fluid, the glucose concentration level in the plasma would increase whenever regulation metabolism dysfunctions. (However, there are actual pathological cases of hypoglycemia, where the malfunction of the regulatory mechanism results in a decreased level of glucose.) Also, utilization of fat and protein will increase in diabetic situations because cells have to find energy from sources other than glucose.

4. Maintenance of blood-glucose level: Mass-flow model

With reference to the process of maintaining blood-glucose levels illustrated in Figure 1, the whole gamut of associated regulatory metabolism, in essence, is decided by mass-flow considerations involving glucose, insulin, and glucagon at appropriate sites in the human body. A classical

https://doi.org/10.25088/ComplexSystems.16.4.343

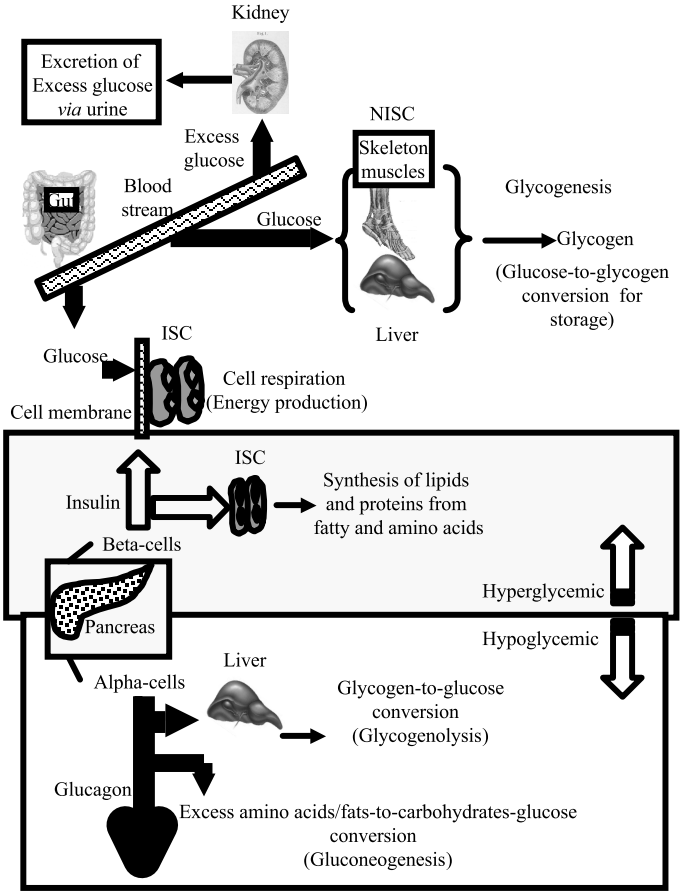

Figure 1. Maintenance of blood-glucose level *via* antagonistic functional roles of insulin and glucagon hormones.

model of such glucose regulation is due to Cobelli and Mari [1, 2], which consists of a metabolic plant made of a glucose controller plus the pair of antagonistic hormonal controllers insulin and glucagon.

Figure 2 shows the relevant architecture of the model depicting mass and control signal flows in the metabolic plant under discussion along with explicit variables in the metabolic plant pertinent to insulin, glucose, and glucagons subsystems that constitute the glucose regulatory process in humans [10].

The glucose subsystem depicted in Figure 2 is a one-compartment model governing the associated flows of extracellular fluids. The underlying processes of this glucose subsystem can be explicitly regarded as functions involving (*i*) net hepatic glucose balance (i.e., the difference between liver glucose production and liver uptake), (*ii*) renal excretion

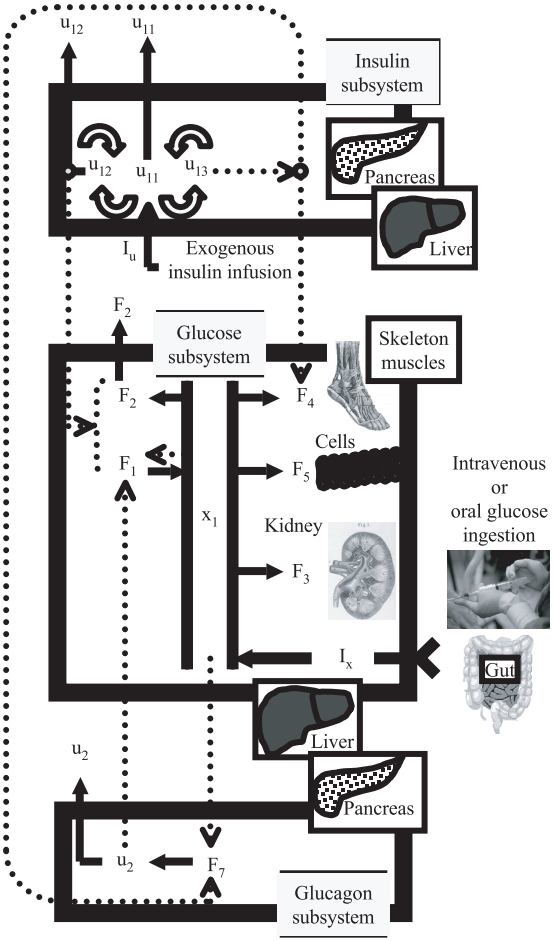

Figure 2. Illustration of explicit variables involved in insulin, glucose, and glucagons subsystems of the glucose regulatory process in humans [1, 2].

of glucose, (*iii*) insulin-dependent glucose utilization (mainly by muscles and adipose tissues), and (*iv*) insulin-independent glucose utilization (largely by the central nervous system and red blood cells).

The variables associated with the insulin subsystem depicted in Figure 2 refer to those stored and promptly realized from the following set: pancreatic insulin, liver and portal plasma insulin, plasma insulin, and insulin in the interstitial fluids.

Lastly, with reference to glucagon, there are three subsystems which interact *via* control signals. The glucagons subsystem with two hormonal controllers and their interaction with the glucose plant are illustrated in Figure 2.

https://doi.org/10.25088/ComplexSystems.16.4.343

5. Model analysis

The glucose regulatory metabolism modeling strategy adopted here uses the notations of [1, 2] with relevant nomenclature as listed below:

x_1 = Quantity of glucose in the plasma and extracellular fluids (mg)
u_{1p} = Quantity of pancreatic, stored insulin (μU)
u_{2p} = Quantity of pancreatic, promptly releasable insulin (μU)
u_{11} = Quantity of insulin in plasma (μU)
u_{12} = Quantity of insulin in the liver (μU)
u_{13} = Quantity of insulin in the interstitial fluids (μU)
u_2 = Quantity of glucagons in the plasma and interstitial fluids (pg).

The equations that describe flow relations in the model of Figure 2 as proposed in [1, 2] are as follows:

$$\frac{dx_1}{dt} = F_1(x_1, u_{12}, u_2) - F_2(x_1, u_{12}) - F_3(x_1) - F_4(x_1, u_{13}) - F_5(x_1) + I_x(t) \qquad x_1(0) = x_{10} \quad (2a)$$

$$\frac{du_{1p}}{dt} = -k_{21}u_{1p} + k_{12}u_{2p} + W(x_1) \qquad u_{1p}(0) = u_{1po} \quad (2b)$$

$$\frac{du_{2p}}{dt} = k_{21}u_{1p} - (k_{12} + k_{02}(x_1))u_{2p} \qquad u_{2p}(0) = u_{2po} \quad (2c)$$

$$\frac{du_{11}}{dt} = -(m_{01} + m_{21} + m_{31})u_{11} + m_{12}u_{12} + m_{13}u_{13} + I_u(t) \qquad u_{11}(0) = u_{11o} \quad (2d)$$

$$\frac{du_{12}}{dt} = -(m_{02} + m_{12})u_{12} + m_{21}u_{11} + k_{02}(x_1)u_{2p} \qquad u_{12}(0) = u_{12o} \quad (2e)$$

$$\frac{du_{13}}{dt} = -m_{13}u_{13} + m_{31}u_{11} \qquad u_{13}(0) = u_{13o} \quad (2f)$$

$$\frac{du_2}{dt} = -h_{02}u_2 + F_7(x_1, u_{13}) \qquad u_2(0) = u_{2o}. \quad (2g)$$

Lastly, the mass-balance relation on the insulin secretion rate is given by:

$$F_6(u_{2p}, x_1) \equiv k_{02}(x_1)u_{2p}. \quad (8)$$

Equation (2a) denotes in essence, a differential equation depicting mass-balance relations of the glucose subsystem with F_1 and F_2 representing the rates of liver glucose production and uptake respectively. (Hence, the *net hepatic glucose balance*, or NHGB is equal to $F_1 - F_2$.) Further, F_3 is the renal excretion rate, F_4 is the rate of peripheral insulin-dependent glucose utilization, and F_5 is the rate of peripheral insulin-independent glucose utilization. Furthermore, the forcing term $I_x(t)$ in equation (2a)

stands for the rate of exogenous glucose appearing in the glucose pool as a result of oral glucose ingestion (or due to intravenous test).

The function $W(x_1)$ in equation (2b) denotes the rate of insulin synthesis controlled by blood-glucose concentration. $I_u(t)$ in equation (2d) is the rate of infusion of exogenous insulin in the plasma compartment. Further, with reference to glycogen dynamics, F_7 in equation (2g) represents the rate of endogenous release of glucagon, (which is implicitly dependent on glucose in plasma and insulin in interstitial fluids). In the set of relations of equation (2), the parameters m_{ij}, h_{ij}, and k_{ij} are constant rate entities (with the unit min^{-1}) except for k_{02}, (which is a function of x_1). The implicit functions F_1 through F_6 and W, in general, can be regarded as nonlinear functions of the independent variables involved, because the associated functional changes would follow logistic pursuits. That is, any change observed in any of the functions cited (for a given incremental change in the independent variable) would depend upon the already prevailing value of that function.

The notion of logistic considerations can be justified from the associated inertial and diffusive properties of the underlying (physical) mass-flows, which implicitly dictate a saturated growth (or an asymptotic decay) of the function (with respect to the independent variable), implying nonlinear characteristics.

By virtue of such nonlinear considerations, equation (2a) depicts a nonlinear differential equation describing mass-balance relations in the glucose subsystem. It can be written more explicitly in terms of a chain-rule based total differential form as follows:

$$\frac{dx_1}{dt} = \left\{ \begin{array}{l} \dfrac{\partial[f_1 - f_2 - f_3 - f_4 - f_5]}{\partial x_1} \times \dfrac{\partial x_1}{\partial t} + \dfrac{\partial[f_1 - f_2]}{\partial u_{12}} \times \dfrac{\partial u_{12}}{\partial t} + \dfrac{\partial[f_1]}{\partial u_2} \\ \quad \times \dfrac{\partial u_2}{\partial t} - \dfrac{\partial[f_4]}{\partial u_{13}} \times \dfrac{\partial u_{13}}{\partial t} - \dfrac{\partial i_x}{\partial t} \end{array} \right\} \quad (3)$$

where

$f_1 =$ Amount of liver glucose production
$\quad \Rightarrow$ Nonlinear function of (x_1, u_{12}, u_2)
$f_2 =$ Amount of liver glucose uptake
$\quad \Rightarrow$ Nonlinear function of (x_1, u_{12})
$f_3 =$ Amount of renal excretion
$\quad \Rightarrow$ Nonlinear function of (x_1)
$f_4 =$ Peripheral insulin-dependent glucose utilized
$\quad \Rightarrow$ Nonlinear function of (x_1, u_{13})
$f_5 =$ Peripheral insulin-independent glucose utilization
$\quad \Rightarrow$ Nonlinear function of (x_1).

https://doi.org/10.25088/ComplexSystems.16.4.343

Further, consistent with the definition of I_x indicated earlier, it follows that,

$$i_x = \int I_x dt \tag{4}$$

where i_x can be regarded as a nonlinear function of time, t. Referring to equation (3), the superimposed nonlinear functions $(f_1 - f_2 - f_3 - f_4 - f_5)$ can be specified by a single nonlinear function $G(x_1)$. This is true in view of the so-called *Tauber–Wiener theorem* [11], which stipulates that the result of superposed nonlinear functions is itself nonlinear. Likewise, $(f_1 - f_2)$ can be identically set equal to another nonlinear function $H(u_{12})$. Hence, equation (3) reduces to:

$$\frac{dx_1}{dt} = \left\{ \begin{array}{l} \dfrac{\partial G}{\partial x_1} \times \dfrac{\partial x_1}{\partial t} + \dfrac{\partial H}{\partial u_{12}} \times \dfrac{\partial u_{12}}{\partial t} + \dfrac{\partial f_1}{\partial u_2} \times \dfrac{\partial u_2}{\partial t} - \dfrac{\partial f_4}{\partial u_{13}} \\ \quad \times \dfrac{\partial u_{13}}{\partial t} - \dfrac{\partial i_x}{\partial t} \end{array} \right\}, \tag{5a}$$

that is,

$$\left[1 - \frac{\partial G}{\partial x_1}\right] \frac{dx_1}{dt} = \left\{ \frac{\partial H}{\partial u_{12}} \times \frac{\partial u_{12}}{\partial t} + \frac{\partial f_1}{\partial u_2} \times \frac{\partial u_2}{\partial t} - \frac{\partial f_4}{\partial u_{13}} \times \frac{\partial u_{13}}{\partial t} - \frac{\partial i_x}{\partial t} \right\},$$

or,

$$\frac{dx_1}{dt} = \frac{\left[\frac{\partial H}{\partial u_{12}} \times \frac{\partial u_{12}}{\partial t} + \frac{\partial f_1}{\partial u_2} \times \frac{\partial u_2}{\partial t} - \frac{\partial f_4}{\partial u_{13}} \times \frac{\partial u_{13}}{\partial t} - \frac{\partial i_x}{\partial t}\right]}{\left[1 - \frac{\partial G}{\partial x_1}\right]}. \tag{5b}$$

6. Glucose regulation dynamics in the complex system domain

In the classical approach due to Cobelli and Mari [1, 2], the dynamics of the given glucose regulation model follow a deterministic (but, interactive) suite. However, in this paper, the dynamics are specified more comprehensively in a complex system domain by taking duly into account stochastical and interactive considerations. The proposed approach now follows.

Suppose the nonlinear (logistic) functions involved in the model under discussion are expressed as general solutions of respective Bernoulli–Riccati differential equations [11, 12]. Then the corresponding solutions can be written in terms of the following explicit functions:

$$\begin{aligned} G(x_1) &= L_{q_s}(x_1) \\ H(u_{12}) &= L_{q_s}(u_{12}) \\ f_1(u_2) &= L_{q_s}(u_2) \\ f_4(u_{13}) &= L_{q_s}(u_{13}) \end{aligned} \tag{6}$$

where $L_{q_s}(\bullet)$ is the Bernoulli–Langevin function [12, 13] with q_s denoting the spatial-order parameter for the governing function indexed by s depicting, (G, H, f_1, or f_4). Applying the theory of interaction stochastics [8] as warranted in complex system analyses, the value of q_s would lie between 1/2 to ∞. This explicitly means that the extent of nonlinear activity involved spans the regime of spatial order from being totally anisotropic (when $q_s \to 1/2$) to totally isotropic (when $q_s \to \infty$) respectively. This applies to the entire stochastical activity of underlying nonlinear processes concerning each variable, (namely, x_1, u_{12}, u_2, and u_{13}) [8]. Further, the function $L_{q_s}(\bullet)$ depicts a logistic sigmoid and q_s decides the slope of the activation when the variable ($\bullet$), namely, the argument of the function, tends to zero [8, 13].

The choice of $L_{q_s}(\bullet)$ with a single parameter, q_s (in denoting the nonlinear activity) is consistent with the underlying, self-regulating (or self-organizing) process associated with each variable under consideration. This is a realistic representation of adaptive control activities in a complex cybernetic system as elaborated in [7, 12].

Therefore, equation (5b) can be rewritten explicitly as follows:

$$\frac{dx_1}{dt} = \frac{\left[L'_{qH}(u_{12})\frac{\partial u_{12}}{\partial t} + L'_{qf1}(u_2)\frac{\partial u_2}{\partial t} - L'_{qf4}(u_{13})\frac{\partial u_{13}}{\partial t} - \frac{\partial i_x}{\partial t}\right]}{[1 - L'_{qG}(x_1)]}, \tag{7a}$$

that is,

$$\begin{aligned}\frac{dx_1}{dt} = &\left[\frac{L'_{qH}(u_{12})}{1 - L'_{qG}(x_1)}\right]\frac{\partial u_{12}}{\partial t} + \left[\frac{L'_{qf1}(u_2)}{1 - L'_{qG}(x_1)}\right]\frac{\partial u_2}{\partial t} \\ &- \left[\frac{L'_{qf4}(u_{13})}{1 - L'_{qG}(x_1)}\right]\frac{\partial u_{13}}{\partial t} - \left[\frac{1}{1 - L'_{qG}(x_1)}\right]\frac{\partial i_x}{\partial t}\end{aligned} \tag{7b}$$

where the prime sign on the Langevin–Bernoulli function denotes differentiation with respect to the argument. Equation (7b) suggests that the rate of glucose flux (x_1) in blood plasma and extracellular fluid is implicitly dictated by the rates of the following:

- Quantity of insulin in the liver (u_{12})
- Quantity of glucagon in the plasma and interstitial fluids (u_2)
- Quantity of insulin in interstitial fluids (u_{13})
- Amount of glucose present due to oral ingestion or intravenous supply.

However, each of these rates are weighted by nonlinear coefficients A_{q_s},

https://doi.org/10.25088/ComplexSystems.16.4.343

B_{q_s}, C_{q_s}, and D_{q_s} where, explicitly,

$$A_{q_s} = \left[\frac{L'_{qH}(u_{12})}{1 - L'_{qG}(x_1)}\right]$$

$$B_{q_s} = \left[\frac{L'_{qf1}(u_2)}{1 - L'_{qG}(x_1)}\right]$$

$$C_{q_s} = \left[\frac{L'_{qf4}(u_{13})}{1 - L'_{qG}(x_1)}\right]$$

$$D_{q_s} = \left[\frac{L'_{1/2}(0)}{1 - L'_{qG}(x_1)}\right].$$

Considering $L_{q_s}(\bullet)$ with $q_s \to 1/2$, it has unity slope at the origin; that is $L'_{1/2}(0) = 1$ in D_{q_s}. Further, it can be noticed that all the coefficients defined are in the general form

$$\left[\frac{L'_{q\alpha}(a)}{1 - L'_{q\beta}(b)}\right]$$

where α and β denote the index s as appropriate and $\{a, b\}$ represents relevant variables involved as arguments.

The slope at the origin of the Bernoulli–Langevin function will range from 1 to 1/3 corresponding to q_s values of 1/2 to ∞ (depicting the range of totally anisotropic disordered state to totally isotropic ordered state respectively) [7, 8]. Therefore, any $L_{q_s}(\bullet)$ is pertinent to an arbitrary state of disorder of anisotropy (between the *extrema* states) and the limiting values of the coefficients A_q, B_q, C_q, and D_q at the bounds are as follows.

- When $q_G \to 1/2$, coefficients $\{A_{q_s}, B_{q_s}, C_{q_s}, \text{and } D_{q_s}\} \to \infty$.
- When $q_G \to \infty$, the coefficients will reduce to the following:

$$A_{q_s} = \frac{3}{2}L'_{qH}(u_{12})$$

$$B_{q_s} = \frac{3}{2}L'_{qf1}(u_2)$$

$$C_{q_s} = \frac{3}{2}L'_{qf4}(u_{13})$$

$$D_{q_s} = \frac{3}{2}L'_{1/2}(0). \tag{7c}$$

In the intermediate range of q_s, namely, $1/2 \le q_s < \infty$, the given coefficients would incline to follow approximately, $1/z(ab)$ law (where z is a linear function of its independent variables, a and b). The $1/z(a, b)$ law indicated results from the algebraic simplification of the Langevin function (and its derivatives used in equation (7c)) leading to the coefficients

$\{A_{q_s}, B_{q_s}, C_{q_s}$, and $D_{qs}\}$ with explicit values as shown. The inverse proportion law of $1/z(a, b)$ indicates that the coefficients in question may significantly influence the underlying processes only for low values of the associated independent variables (a and/or b); and, these coefficient functions would asymptotically tend to zero for large values of their arguments. Physically, this implies that the nonlinear aspect of the rate of change in regulatory variables would be significant for levels of enzymatic doses present in the system during the early regime of the temporal discourse. However, at a later stage (i.e., towards terminal dynamics), such variations would tend to cease depicting more or less an invariant state of flow of the participant fluxes, namely glucose, glucagons, and insulin. Thus, the regulatory metabolism under consideration refers to an intense (or significantly observable) variant of the *in vivo* activity (dynamic) mostly during the early stages of the processes involved.

7. Model validation: Analytical considerations

Available in [1, 2] is a set of data on glucose and insulin present in the blood of a nondiabetic adult subject (of about a normal weight of 70 kg). These data were obtained after an *oral glucose tolerance test* (o.g.t.t.) on the subject. (The o.g.t.t. is done as follows: After an overnight fast, the subject drinks a solution containing a known amount [100 g] of glucose. A blood sample is obtained before the subject drinks the glucose solution and is tested for its glucose level. Subsequently, blood is drawn every 30 to 60 minutes for up to three hours. The glucose level in each sample is assayed and recorded.) The indicated data set (available in [1, 2]) corresponds to the following: (*i*) The time-course of glucose and insulin plasma concentration for a long oral glucose load, (*ii*) shape and integral data on the glucose rate of appearance in plasma, and (*iii*) disposal of the glucose load among various tissues (i.e., in the liver and in peripheral tissues). A submodel derived thereof has yielded results on unit processes F_1, F_2, and F_4 with approximate values as shown in Tables 1, 2, and 3 (corresponding to the results in [1, 2]). The clinical (procedural) details of these tables are as indicated in [1, 2].

Relevant to the data in Tables 1 through 3, the model under consideration depicted *via* equation (7) can be verified as follows. The associated expression of equation (7) can be rewritten as:

$$\frac{dx_1}{dt} = A_{q_s}\frac{du_{12}}{dt}\bigg|_{u_2} + B_{q_s}\frac{du_2}{dt}\bigg|_{u_{12}} - C_{q_s}\frac{du_{13}}{dt}\bigg|_{u_2,u_{12}} - D_{q_s}\frac{di_x}{dt}\bigg|_{u_2,u_{12},u_{13}} \tag{8a}$$

where, as indicated before, the subscript q_s on the coefficients explicitly depicts the spatial-order parameter associated with the variables involved; and, q_s equal to 1/2 and ∞ specifies the extreme (upper and lower) bounds on the stochastical variations of the variables. Further,

https://doi.org/10.25088/ComplexSystems.16.4.343

	Liver insulin concentrations (μU/ml): u_{12}			
	10	100	200	300
Glucose concentration (mg/dl) (x_1)	Liver glucose production (mg/min kg) (F_1)			
50	4.65	1.70	0.45	0.04
60	4.63	1.70	0.45	0.04
70	4.60	1.68	0.44	0.04
80	4.50	1.65	0.42	0.04
90	4.20	1.54	0.40	0.04
100	3.20	1.20	0.32	0.02
110	2.10	0.73	0.20	0.01
120	1.00	0.38	0.10	0.01
130	0.35	0.15	0.03	0.01
140	0.13	0.05	0.02	0.01
150	0.05	0.03	0.01	0.01
160	0.01	0.01	0.01	0.01
170	0.01	0.01	0.01	0.01
Glucagon concentration (u_2) = 0.075 ng/ml				

Table 1a. Data on Liver glucose production (F_1) in mg/min kg *versus* glucose concentration (x_1) in mg/dl for a given glucagon concentration of 0.075 ng/ml and at different liver insulin concentration levels (μU/ml) [1, 2] obtained in the o.g.t.t.

equation (8a) is constrained by initial and terminal values of the rate dx_1/dt. The numerical values of such initial/terminal conditions are explicitly available in the experimental data of Tables 1 through 3 [1, 2].

Considering an adult subject (70 kg), on the approximate trend of the rate of appearance of glucose (namely, $|dx_1/dt|$) in plasma (after an o.g.t.t.) *versus* time can be specified in terms of the deterministic values of experimental observations [2, 3]. Such a trend is reproduced here as Figure 3 for convenient reference.

Marked on Figure 3 are four time phases. Phase I depicts the glucose rate of appearance ($|dx_1/dt|$, due to glucose infusion facilitated *via* o.g.t.t.) starting at an initial condition of $t = 0$ and terminating at $t = t_{\mathrm{I}}$, where the glucose rate of appearance starts falling into Phase II with a specified slope and ending at $t = t_{\mathrm{II}}$. In Phase III, the glucose rate of appearance continues to fall but at a different slope. Lastly, in Phase IV $|dx_1/dt|$ as a function of time tends to cease from the approximate instant $t = t_{\mathrm{III}}$ marking the cessation of o.g.t.t. across the terminal phase.

Our model is concerned with validating Phase II and onwards described by the complex system stochastics depicted *via* equation (8a). Phase I is omitted since it denotes only the transient event of glucose

	Liver insulin concentrations (μU/ml): u_{12}			
	10	100	200	300
Glucose concentration (mg/dl) (x_1)	Liver glucose production (mg/min kg) (F_1)			
50	6.60	2.35	0.6	0.08
60	6.55	2.34	0.6	0.08
70	6.50	2.32	0.58	0.08
80	6.30	2.30	0.57	0.08
90	5.90	2.20	0.55	0.08
100	5.00	1.83	0.45	0.07
110	3.60	1.30	0.30	0.05
120	1.80	0.63	0.20	0.05
130	0.70	0.30	0.10	0.05
140	0.25	0.10	0.07	0.05
150	0.10	0.07	0.05	0.05
160	0.05	0.05	0.05	0.05
170	0.05	0.05	0.05	0.05
Glucagon concentration (u_2) = 0.160 ng/ml				

Table 1b. Liver glucose production (F_1) in mg/min kg *versus* glucose concentration (x_1) (mg/dl) for a given glucagon concentration of 0.160 ng/ml and at different liver insulin concentration levels (μU/ml) [1, 2] obtained in the o.g.t.t.

	Liver insulin concentrations (μU/ml): u_{12}			
	10	100	200	300
Glucose concentration (mg/dl) (x_1)	Liver glucose uptake (mg/min kg) (F_2)			
50	0.03	0.30	3.35	7.45
60	0.03	0.30	3.35	7.45
70	0.03	0.30	3.35	7.45
80	0.03	0.30	3.35	7.45
90	0.04	0.30	3.35	7.45
100	0.10	0.39	3.40	7.80
110	0.30	0.70	3.60	8.50
120	0.95	1.30	4.30	8.85
130	1.35	1.65	4.70	8.95
140	1.43	1.70	4.80	8.97
150	1.44	1.72	4.80	8.97

Table 2. Liver glucose uptake (F_2) (in mg/min kg) *versus* glucose concentration (x_1) in mg/dl at different levels of liver insulin concentrations [1, 2] obtained in the o.g.t.t.

https://doi.org/10.25088/ComplexSystems.16.4.343

	Interstitial fluid insulin concentrations (μU/ml): u_{13}			
	10	100	200	300
Glucose concentration (mg/dl) (x_1)	Peripheral glucose uptake (mg/min kg) (F_4)			
50	0.20	1.9	9.1	12.0
60	0.30	1.3	11.0	14.5
70	0.40	2.9	13.0	17.8
80	0.45	3.3	15.5	20.7
90	0.55	3.9	18.8	24.0
100	0.60	4.2	21.0	27.5
110	0.61	4.9	23.8	30.5
120	0.65	5.3	26.0	33.5
130	0.70	5.9	28.0	36.6
140	0.80	6.0	30.0	38.8
150	0.80	6.5	31.5	40.6
160	0.80	6.8	32.6	42.1
170	0.80	7.0	33.5	43.5
180	0.80	7.0	34.2	44.3
190	0.80	7.1	35.0	45.1
200	0.80	7.2	35.5	45.9
210	0.80	7.3	35.9	46.2
220	0.80	7.4	36.2	46.8
230	0.80	7.5	36.5	47.0
240	0.80	7.5	36.7	47.1
250	0.80	7.5	36.9	47.3

Table 3. Peripheral glucose uptake (F_4) in mg/min kg *versus* glucose concentration (x_1) in mg/dl at different interstitial fluid insulin concentrations [1, 2] obtained in the o.g.t.t.

appearance caused by o.g.t.t. initiation. As such, only the actual metabolic activity that sets in subsequently through Phase II and beyond is modeled in the present effort. Hence, denoting the value of $D_q[di_x/dt]_{u_2,u_{12},u_{13}}$ in equation (8a) as equal to K_{I} at $t = t_{\mathrm{I}}$ and as K_{II} at $t = t_{\mathrm{II}}$ (with explicit numerical values for K_{I} and K_{II} in Table 1), equation (8a) can be specified in terms of initial and final (terminal) conditions of Phases II and III as follows:

$$\left[\frac{dx_1}{dt}\right]_{t=t_{\mathrm{I}}} = -K_{\mathrm{I}} \tag{8b}$$

and

$$\left[\frac{dx_1}{dt}\right]_{t=t_{\mathrm{II}}} = -K_{\mathrm{II}}. \tag{8c}$$

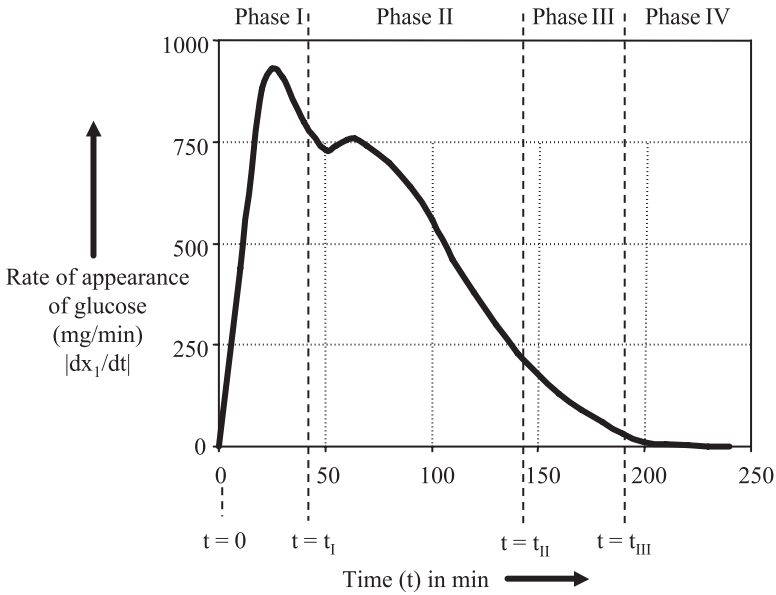

Figure 3. Rate of appearance of glucose $|(dx_1/dt)|$ as a function of time [1, 2] after a 100 g, o.g.t.t.

Hence normalizing equation (8a) and attributing the initial and final values of the time course of $|dx_1/dt|$ with the coefficients K_{I} and K_{II}, it follows that

$$1 - \left[\frac{\left(\left| \frac{dx_1}{dt} \right| \right)_t}{\left(\left| \frac{dx_1}{dt} \right| \right)_{t=t_1}} \right] \times K_{\mathrm{I}}, \qquad t_{\mathrm{I}} \le t \le t_{\mathrm{II}}$$

and

$$1 - \left[\frac{\left(\left| \frac{dx_1}{dt} \right| \right)_{t_t}}{\left(\left| \frac{dx_1}{dt} \right| \right)_{t=t_1}} \right] \times K_{\mathrm{II}}, \qquad t_{\mathrm{II}} \ge t \ge t_{\mathrm{III}} \tag{8d}$$

where $(|dx_1/dt|)_t = A_q[du_{12}/dt]_{u_2} - B_q[du_2/dt]_{u_{12}} - C_q[du_{13}/dt]_{u_2,u_{12},u_{13}}$.

To compute equation (8d), the time-course functions (du_{12}/dt) and (du_2/dt) should be evaluated. However, the data available in [1, 2], (and reproduced here in Tables 1 through 3) denote the discourses of relevant variables with respect to x_1 (and not with respect to time, t). Therefore, the following transformations are needed:

$$\left.\frac{du_{12}}{dt}\right|_{u_2} = \frac{du_{12}}{dx_1} \cdot \left.\frac{dx_1}{dt}\right|_{u_2} = F_1 \left.\frac{du_{12}}{dx_1}\right|_{u_2} \tag{9a}$$

$$\left.\frac{du_2}{dt}\right|_{u_{12}} = \frac{du_2}{dx_1} \cdot \left.\frac{dx_1}{dt}\right|_{u_{12}} = F_1 \left.\frac{du_2}{dx_1}\right|_{u_{12}} \tag{9b}$$

https://doi.org/10.25088/ComplexSystems.16.4.343

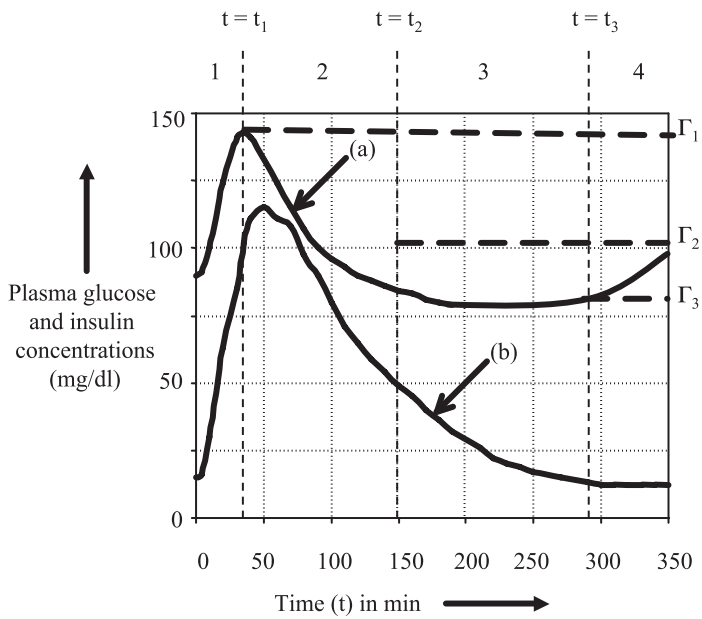

Figure 4. Approximate glucose and insulin concentrations in normal subjects after a 100 g, o.g.t.t. [1, 2]: (a) plasma glucose (x_1) and (b) plasma insulin.

and

$$\left.\frac{du_{13}}{dt}\right|_{u_2,u_{12}} = \frac{du_{13}}{dx_1}\cdot\left.\frac{dx_1}{dt}\right|_{u_2,u_{12}} = F_4\left.\frac{du_{13}}{dx_1}\right|_{u_2,u_{12}}. \tag{9c}$$

The expressions of equation (9) can now be computed using the data of Tables 1 through 3. Further, the integration of equation (8a) leads to:

$$x_1(t) = A_q u_{12}(t) + B_q u_2(t) - C_q u_{13}(t) - D_q i_x(t) + C_o \tag{10}$$

where C_o is a constant of integration.

Again, when equation (10) is subjected to initial and terminal conditions consistent with the data of [1, 2], the constant of integration can be decided explicitly. For this purpose, the plasma glucose concentration *versus* time observed in normal subjects (after a 100 g, o.g.t.t.) as available in [1, 2], is considered. Relevant data is presented in Figure 4 where there are four distinct regimes of time. Phase 1 depicts the onset of plasma glucose appearance reaching a peak value. Thereupon, x_1, (namely, the plasma glucose concentration) falls with respect to time across Phase 2; then, this rate of fall decreases as in Phase 3. Subsequently, the concentration of plasma glucose shows an ascending trend in Phase 4. The present study specifically models the time-discourse of plasma glucose concentration across Phase 2 and onwards. Again,

Phase 1 depicts only the transient rise in glucose level as a result of o.g.t.t. initiated on the subject. Therefore, it is omitted and only the actual metabolic activity that sets in through Phase 2 and beyond is modeled.

The initial ($t = \tau_1$) and terminal ($t = \tau_2$) conditions of equation (10) denote the onset and end of Phase 2 as shown in Figure 4 where, at $t = \tau_1$, $x_1(t = \tau_1) = \Gamma_1$ and at $t = \tau_2$, $x_1(t = \tau_2) = \Gamma_2$ as marked. Considering the epoch of Phase 2, modeled *via* equation (10), the associated functions $u_{12}(t)$, $u_2(t)$, and $u_{13}(t)$ can be determined as outcomes of appropriate integrations (with the initial and terminal conditions specified respectively by: $t = \tau_1$, $x_1(t = \tau_1) = \Gamma_1$ and at $t = \tau_2$, $x_1(t = \tau_2) = \Gamma_2$. For example, considering u_{12}, it can be ascertained by the following integration (or summation):

$$\int \left[\frac{du_{12}}{dt}\right]_{u_2} dt = \int \left[\frac{du_{12}}{dx_1} \cdot F_1\right]_{u_2} dt$$
$$= \left[\sum_i \left[\frac{(\Delta u_{12})_i}{(\Delta x_1)_i}\right] \times (F_1)_i \times (\Delta t)_i\right]_{u_2} \tag{11a}$$

where i denotes the running variable in a summation process (*in lieu* of integration) across $\tau_1 \le t \le \tau_2$ subdivided into i segments with each segment having a length of Δt_i. The summation indicated enables numerical integration with $(\Delta x_1)_i$ depicting the ith segment length along the x_1-axis corresponding to Δt_i in the time scale; and, F_{1_i} represents the value of F_1 at segment i. Lastly, $(\Delta u_{12})_i$ is the differential change in u_{12} along time, t.

The experimental data in Table 1(a) is used for computing equation (11a), which offer the following explicit numerical values. Given $u_2 = 0.075$ ng/ml, the values $u_{12} = 10$ μU/ml and $u_{12} = 100$ μU/ml leads to $\Delta u_{12} = -90$ μU/ml, (which remains constant throughout x_1 discourse). That is, in the relevant computations, $\Delta u_{12} = -90$ μU/ml is adopted. Similarly, considering Table 1(b) data (for $u_2 = 0.160$ ng/ml), again, $\Delta u_{12} = -90$ μU/ml.

Following similar algorithmic considerations, u_2 and u_{13} can be specified as follows:

$$\int \left[\frac{du_2}{dt}\right]_{u_{12}} dt = \int \left[\frac{du_2}{dx_1} \cdot F_1\right]_{u_{12}} dt$$
$$= \left[\sum_i \left[\frac{(\Delta u_2)_i}{(\Delta x_1)_i}\right] \times (F_1)_i \times \Delta t_i\right]_{u_{12}} \tag{11b}$$

https://doi.org/10.25088/ComplexSystems.16.4.343

and,

$$\int \left[\frac{du_{13}}{dt}\right]_{u_2,u_{12}} dt = \int \left[\frac{du_{13}}{dx_1} \cdot F_4\right]_{u_2,u_{12}} dt$$
$$= \left[\sum_i \left[\frac{(\Delta(u_{13})_i}{(\Delta x_1)_i}\right] \times (F_4)_i \times (\Delta t)_i\right]_{u_2,u_{12}} . \qquad (11c)$$

Again, for explicit computation of equation (11b), the data sets of Tables 1(a) and 1(b) can be used; and, likewise the underlying computation of equation (11c) can be identified with the data set of Table 3.

8. Model validation: Computations and results

As mentioned earlier, in order to compute equations (9) and (11) (and for subsequent evaluation of equations (8) and (10)), the data required are provided in Tables 1 through 3.

In the computational procedure, for each differential span of Δt_i over the different phases of the time interval (between initial and terminal events), the corresponding Δx_i is taken from the tables and relevant (F_{1i}) and (F_{4i}) at this Δx_i segment are determined. Hence, the parameters $u_{12}(t)$, $u_2(t)$, and $u_{13}(t)$ are elucidated at that differential time segment of Δt_i. Thus, the accumulated values of Δx_i (depicting the numerical integration over successive segments of Δt_i), the values of $|dx_1/dt|$ and $x_1(t)$ are computed using the coefficients A_{q_s}, B_{q_s}, C_{q_s}, and D_{q_s} that were evaluated as indicated earlier. For each ensemble of such computations, the q_s value is picked randomly from a uniformly distributed set of numbers (from 1/2 to a large value, theoretically tending to ∞). Using the ensemble of computational runs of the simulations yields the unbiased stochastical variations involved in the time-course of the functions $|dx_1/dt|$ and $x_1(t)$.

The assumed random variations justifiably prevail in the complex interactive domain of the process under consideration; and, the range of disorder involved is specified within the selected bounds of $q_s = 1/2$ to $q_s \to \infty$. In the simulations performed, however, for values of q_s larger than 10, the results remained almost invariant, implying that the lower bound has almost been reached when $q_s \approx 10$.

Further, using the relevant numerical values of initial and terminal conditions in Tables 1 through 3 the normalized values of $|dx_1/dt|$ and $x_1(t)$ are established. That is, the values of the sets $\{K_{\mathrm{I}}, K_{\mathrm{II}}, K_{\mathrm{III}}\}$ and $\{\Gamma_1, \Gamma_2, \Gamma_3\}$ are gathered from the tables at the epochs of time. Further, appropriate scaling is done to render the explicit values for the constants of integration in a normalized form. The computed results on $|dx_1/dt|$ and $x_1(t)$ are presented in Figures 5 and 6 respectively.

Shown as error bars, the lower bound in Figure 5 is close to the experimental data and the upper bound is about 15% higher than the

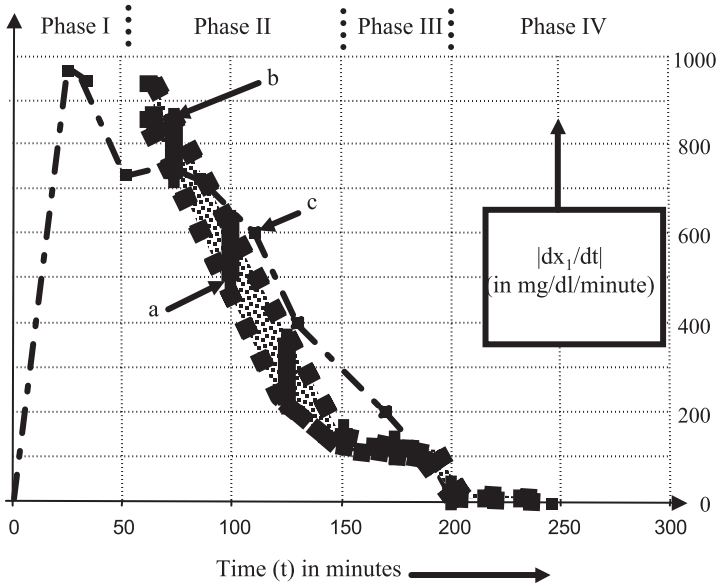

Figure 5. Rate of appearance of glucose $|(dx_1/dt)|$ *versus* the passage of time in the 100 g, o.g.t.t. regimen on a normal (70 kg) adult. Simulated results of the proposed complexity model: Cluster of random data obtained corresponding to various values of q_s, randomly chosen (with uniform distribution) between 1/2 and a large value (≥10) depicting (a) upper and (b) lower bounds. (c) Is the Measured data from [1, 2].

experimental values. In Figure 6, the upper bound is closer to the clinical data in Phase II and deviates by 12% in the rest of the time scale. The lower bound is around 10% below the experimental values. These computed bounds can be regarded to be within close ranges of tolerance taking into account experimental dispersions that may exist.

9. Inferential remarks

This study implies that a complex system approach is needed to account duly for the stochastical considerations in modeling metabolic regulatory processes, where the associated interactions between various subsystems should (at least) be approximately accounted for in the spatiotemporal domain. The present study is an exemplary effort to profile the glucose regulatory metabolism; and, modeling efforts give due considerations to assert the interactions between subsystems and the stochastical aspects of the parameters involved. Starting from the deterministic model of mass-balance relations pertinent to glucose regulatory metabolism due to Cobelli and Mari [1, 2], necessary modifications are done to include comprehensively the required complex system consider-

https://doi.org/10.25088/ComplexSystems.16.4.343

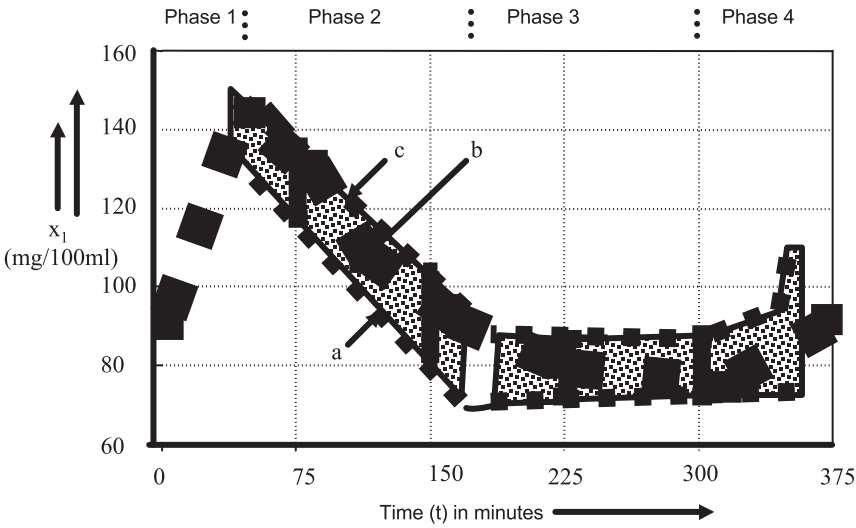

Figure 6. Plasma glucose concentration (x_1) *versus* the passage of time in the 100 g, o.g.t.t. regimen on a normal (70 kg) adult. Simulated results of the proposed complexity model: Cluster of random data obtained corresponding to various values of q_s, randomly chosen (with uniform distribution) between 1/2 and a large value (≥10) depicting (a) upper and (b) lower bounds. (c) Is the measured data from [1, 2].

ations. It can be stated that the efforts of Cobelli and Mari [1, 2] address a complex system of deterministic notions and interactive dynamics, but they describe the system dynamics by a set of very complicated equations comprising seven variables, more than 10 functions, and around 50 adjustable constants. However, the present complex system model is to a large extent simpler involving only four variables.

The complex regulation dynamics developed here follow a logistic temporal trend as decided by a Bernoulli–Riccati nonlinear differential equation [12, 13], which models the regulation dynamics with an explicit self-regulating (self-organizing) nonlinearity expressed in the complex cybernetic domain of interactions (with probabilistic attributes) *via* a spatial-order parameter under probabilistic notions.

Considering practical values of clinical significance, simulations are performed on the model developed to elucidate the dynamics of glucose rate of appearance and plasma glucose concentration. The simulated results follow the existing experimental results across upper and lower bound limits of the system output (*versus* time) as illustrated in Figures 5 and 6. It is observed that in the region of randomly simulated results (on x_1 and $|dx_1/dt|$ *versus* time), are the clinical observations contained between a pair of upper and lower bounds. This validates the hypothesis on complex system considerations presumed.

10. Closure

Most bio-system processes normally follow nonlinear dynamic pursuits and exhibit stochastical and deterministic attributes. Further, their constitutive subsystems interact dynamically with the underlying activities seeking a convergence through cybernetic feedback. As such, bio-system activities, in general, comply with the norms of complex system considerations. The associated complexity in this study is expressed quantitatively by $C(t)$ of equation (1) depicting the dependence of complexity on a large number of constituent elements (n), their variety (N). The functional aspect of (n, N) denoted by ϕ in equation (1) refers explicitly to the dynamics of x_1 and dx_1/dt in the context of glucose metabolism.

A typical use of the study performed would be in adaptively refining an insulin infusion pump algorithm used in the controlled delivery of insulin by means of a release pump. In this technique (known as the insulin pump therapy [4–6, 14]), the size of the pump worn by a subject is that of a pager. This pump is programmed to deliver a continuous flow of insulin at a low basal rate through a subcutaneous needle. After meals, the injection rate may correspond to a larger bolus rate. Further, in order to achieve good blood glucose control, the insulin delivery/infusion programmed into the system should conform closely to the time-schedule profile of the glucose metabolism involved. Normally, it is difficult in practice to "tune" the system for a given subject with a rigidly specified deterministic profile of the underlying metabolic activity that can be adaptively matched to the time excursion of the activity and control the insulin infusion regimen [10]. However, the model on glucose metabolism developed here provides a region of spread set between upper and lower bounds on the associated dynamics taking into consideration stochastical variations and interaction parameters involved. Within these bounds the algorithm in question can also be specified in terms of fuzzy norms in view of the deliberations given in [15–17]. Relevant analytical considerations can be lucidly introduced in the infusion pump algorithm (*in lieu* of a rigidly imposed deterministic rule) for a more robust track-and-infuse operation of the insulin pump. Relevant work on fuzzy considerations are in progress.

References

[1] C. Cobelli and A. Mari, "Validation of Mathematical Models of Complex Endocrine-Metabolic Systems. A Case Study on a Model of Glucose Regulation," *Medical and Biological Engineering and Computing*, **21** (1983) 390–399.

[2] C. Cobelli and A. Mari, "Control of Diabetes with Artificial Systems for Insulin Delivery: Algorithm Independent Limitations Revealed by a

https://doi.org/10.25088/ComplexSystems.16.4.343

Modeling Study," *IEEE Transactions on Biomedical Engineering*, **BME-32** (1985) 840–845.

[3] J. T. Sorensen, *A Physiologic Model of Glucose Metabolism in Man and Its Use to Design and Assess Improved Insulin Therapies for Diabetes* (Doctor of Science Thesis, Department of Chemical Engineering, Massachusetts Institute of Technology, 1985).

[4] R. B. Northrop and E. A. Wooddruff, "Regulation of a Physiological Parameter or *in vivo* Drug Concentration by Integral Pulse Frequency Modulated Bolus Drug Injections," *IEEE Transactions on Biomedical Engineering*, **BME-33** (1986) 1010–1020.

[5] R. S. Parker, F. J. Doyle III, and N. A. Peppas, "A Model-based Algorithm for Blood Glucose Control in Type I Diabetic Patients," *IEEE Transactions on Biomedical Engineering*, **46** (1999) 148–157.

[6] C. Deeney, "Insulin Therapy by Continuous Subcutaneous Infusion," *The Pharmaceutical Journal*, **271** (2003) 206–208.

[7] P. S. Neelakanta, J. C. Park, and D. De Groff, "Complexity Parameter *vis-à-vis* Interaction Systems: Applications to Neurocybernetics," *Cybernetica*, **XL** (1997) 243–253.

[8] P. S. Neelakanta and D. De Groff, *Neural Network Modeling: Statistical Mechanics and Cybernetic Principles* (CRC Press, Boca Raton, FL, 1994).

[9] V. C. Scalon and T. Sanders, *Essentials of Anatomy and Physiology* (F. A. Davis Company, Philadelphia, PA, 2003).

[10] M. C. K. Khoo, *Physiological Control Systems: Analysis Simulation and Estimation* (IEEE Press, Piscataway, NJ, 1999).

[11] P. S. Neelakanta (ed.), *Information-theoretic Aspects of Neural Networks* (CRC Press, Boca Raton, FL, 1999).

[12] P. S. Neelakanta, S. Abusalah, D. De Groff, and R. Sudhakar, "Logistic Model of Nonlinear Activity in a Neural Complex: Representation *via* Riccati Differential Equation," *Cybernetica*, **XXXIX** (1996) 15–30.

[13] P. S. Neelakanta, R. Sudhakar, and D. De Groff, "Langevin Machine: A Neural Network Based on Stochastically Justifiable Sigmoidal Function," *Biological Cybernetics*, **65** (1991) 331–338.

[14] D. G. Allen and M. V. Sefton, "A Model of Insulin Delivery by a Controlled Release Micropump," *Annals of Biomedical Engineering*, **14** (1986) 257–276.

[15] M. Hanss and O. Nehls, "Simulation of Human Glucose Metabolism Using Fuzzy Arithmetic," *Proceedings of the Nineteenth International Conference of the North American Fuzzy Information Processing Society* (NFIPS, 13–15 July 2000), pp. 201–205.

[16] M. Hanss and O. Nehls, "Enhanced Parameter Identification for Complex Biomedical Models on the Basis of Fuzzy Arithmetic," *Proceedings of the Joint IFSA World Congress and Twentieth NAFIPS International Conference* (25–28 July 2001), **3** (2001) 1631–1636.

[17] M. Mahfouf, M. F. Abbod, and D. A. Linkens, "A Survey of Fuzzy Logic Monitoring and Control Utilisation in Medicine," *Aritificial Intelligence in Medicine*, **21** (2001) 27–42.

https://doi.org/10.25088/ComplexSystems.16.4.343